

# Bioactive double glass coatings for Co–Cr–Mo alloy

Ö. H. ANDERSSON<sup>‡</sup>, K. H. KARLSSON

*Department of Chemical Engineering, Åbo Akademi University, FIN-20500 Åbo/Turku, Finland*

H. HERO

<sup>‡</sup>NIOM, Scandinavian Institute of Dental Materials, N-1344 Haslum, Norway

E. VEDEL, A. YLI-URPO

*Institute of Dentistry, University of Turku, FIN-20520 Turku/Åbo, Finland*

K. J. J. PAJAMÄKI, T. S. LINDHOLM

*Department of Clinical Sciences, University of Tampere, FIN-33520 Tampere, Finland*

Glass compositions for double coatings for a Co–Cr–Mo alloy were developed. The glass compositions were chosen to fulfil such requirements as matching thermal expansion, low glass transition temperature and moderate solubility. For the ground coat a fairly high durability is required, whereas the cover coat must be bioactive, i.e. become attached to living bone by a chemical bond. Two compositions of each type were developed by computer-aided optimization. The glasses were chosen in the  $\text{Na}_2\text{O}-\text{CaO}-\text{B}_2\text{O}_3-\text{Al}_2\text{O}_3-\text{SiO}_2-\text{P}_2\text{O}_5$  system. The bioactivity was tested *in vitro* by immersion in a simulated body fluid. The double coatings on Co–Cr–Mo alloy released hexavalent chromium into the solution as detected by yellow colouration and spectrophotometry. This colouration was strong at the margin between coated and uncoated metal and may be explained by oxidation of trivalent chromium of the alloy in the presence of glass. The released chromium did not have any notable effect on the calcium phosphate formation. After replenishing the solution no coloration was observed. This suggests that the chromate is easily dissolved and that it may be possible to wash it out prior to implantation.

## 1. Introduction

A number of studies deal with bioactive glass coatings. For example coating of alumina [1–4], stainless steel [5–8], Co–Cr–Mo alloy [9–11] and titanium [12], have been reported. All systems seem to have deficiencies. A coating with good bone bonding can be obtained by rapid immersion of the prosthesis in molten glass. However, the rapid immersion technique gives a thick coating. To take full advantage of the reinforcing effect of the metal, the coating should be as thin as possible.

For a good result a number of properties of the coating must be controlled. In contact with body fluid bioactive glasses undergo reactions which result in the formation of a sub-surface Si-rich layer (Si-gel) and a Ca,P-rich surface layer. The Si-gel layer forms due to leaching of ions from the glass. With time the Si-gel grows in thickness, which decreases its strength. Thus, it is desirable to decrease the solubility of the bioactive glass as much as possible without losing bioactivity. If the leaching progresses to the glass–metal interface the glass might scale off due to loss of adhesion. One way to avoid this problem is to use a durable ground coat. The ground coat ideally also protects the bioactive cover coat from contamination by metal ions which may dissolve from

the substrate during firing. Ions which dissolve from the substrate into the coating may inhibit bone bonding [13].

$\text{Al}_2\text{O}_3$  may be added to increase the stability of the ground coat. There are, however, reports on disturbance of osteoid mineralization in the presence of glasses containing  $\text{Al}_2\text{O}_3$  [14, 15]. It is also known that alumina may interfere with calcium phosphate formation at the glass surface. Andersson *et al.* [16] reported a three-fold increase in the alumina content at the glass surface as compared with bulk glass, after implantation for 8 weeks in rabbit tibia. This alumina enrichment completely inhibited calcium phosphate formation and consequently bone bonding. Greenspan and Hench [1] coated an alumina ceramic with bioactive glass. Firing temperatures above 1100 °C were used and the reaction behaviour of the glass was affected by dissolution of alumina into it. Thus, it is important to avoid extensive diffusion of alumina from the ground coat into the bioactive cover coat. To minimize diffusion the ground coat should have a low alumina content, the firing temperature should be low and the time short.

The compressive strength of a glass is far greater than its tensile strength. In order to obtain compression in the glass the thermal expansion ( $\alpha$ ) of the glass

should be slightly lower than that of the metal. However, if  $\alpha$  of the glass is too low the glass scales off when cooled. The glass transition temperature ( $T_g$ ) should be low for both ground and cover coat.  $T_g$  of the ground coat should, however, be higher than, or at least about the same as, that of the cover coat.

To develop glasses which meet a set of prespecified properties is a typical problem of optimization [17, 18]. The purpose of the present work was to develop, by compositional optimization, double glass coatings for a Co–Cr–Mo prosthesis and to test their bioactivity *in vitro*.

## 2. Materials and methods

A Co–Cr–Mo alloy (Wirobond, BEGO Bremer Goldschlägerei Wilh. Herbst GmbH & Co., Bremen, FRG) was cast at 1470 °C into rods with a diameter of 6 mm. The rods were cut with a diamond saw to 1 mm discs. The thermal expansion of the alloy is, according to the manufacturer,  $14.7 \times 10^{-6} \text{ K}^{-1}$ .

Four glass compositions were developed by compositional optimization. The method is described in Appendix 1. The glasses were of two types. Non-active  $\text{Al}_2\text{O}_3$ -containing glasses were designed for durable ground coats (G1, G2) and  $\text{Al}_2\text{O}_3$ -free bioactive glasses (C1, C2) for cover coats (Table I). G1 was always coated with C1 and G2 with C2. In optimizing the glasses, thermal expansion, glass transition temperature, bioactivity, and solubility were considered. For the thermal expansion coefficient Appen's method was used [19]. Previously published models were used for glass transition temperature [20] and bioactivity [16, 21]. The solubility is expressed as the amount (ml) of 0.01 M HCl consumed to maintain the pH at 7.4 in 100 ml aqueous 15 mM Na-citrate solution, during a 60 min immersion of 200 mg glass grains (297–500  $\mu\text{m}$ ). The optimization data and the predicted properties are given in Appendix 1.

TABLE I Glass compositions by synthesis (wt %)

	Oxide					
	$\text{Na}_2\text{O}$	$\text{CaO}$	$\text{B}_2\text{O}_3$	$\text{Al}_2\text{O}_3$	$\text{SiO}_2$	$\text{P}_2\text{O}_5$
G1	25.84	10.24	0.00	3.00	59.62	1.30
C1	24.42	12.99	1.83	0.00	55.86	4.90
G2	23.00	10.00	0.00	3.00	64.00	0.00
C2	21.10	20.00	1.60	0.00	57.30	0.00

TABLE II Samples tested by immersion in SBF for 72 h at 37 °C

Metal	Glass	Total coat thickness	Firing
–	C1	–	–
–	C2	–	–
Co–Cr–Mo	C1	5 $\mu\text{m}$	640 °C/30 min
Co–Cr–Mo	C2	5 $\mu\text{m}$	700 °C/20 min
Co–Cr–Mo	G1 + C1	200–300 $\mu\text{m}$	680 °C/20 min + 640 °C/30 min
Co–Cr–Mo	G2 + C2	200–300 $\mu\text{m}$	750 °C/10 min + 700 °C/20 min

The glasses (Table I) were melted at 1360 °C for 3 h. Part of the batch was cast in graphite and annealed at the predicted  $T_g$  (Appendix 1) to produce bulk samples, and part was quenched in water. The quenched glass was milled, sieved to a particle size of less than 45  $\mu\text{m}$  and dispersed in ethanol.

The alloy specimens were dipped in this frit and subsequently dried. Room-temperature specimens were inserted directly to the firing temperature. Firing was done in ambient atmosphere. In order to find suitable firing schemes resulting in dense coats, pulverized samples of the different compositions were individually heat-treated at 570–750 °C for 10–60 min on platinum foil. The firing scheme for each coat was chosen so as to minimize temperature and time. The diffusion of aluminium from the ground coat into the cover coat (mixing zone) was investigated by scanning electron microscopy (SEM) and energy dispersive X-ray analysis (EDXA). These analyses were done on ground (600 grit) cross-sections of epoxy-embedded samples. The depth of diffusion was taken as the depth at which the aluminium signal disappeared when going from ground to cover coat.

Differential thermal analysis (DTA) was performed on pulverized glass at a heating rate of 20 °C  $\text{min}^{-1}$ . The sample mass was 50 mg and  $\text{Al}_2\text{O}_3$  was used as a reference.

The bioactivity was tested at 37 °C by studying the formation of calcium phosphate at the glass surface in a tris-buffered simulated body fluid (SBF) [23] which contains inorganic ions in concentrations close to those in human plasma [24]. If calcium phosphate formed the material was assumed to be bioactive. Bulk glass as well as coated alloy samples were studied (Table II). Prior to testing, the samples were ultrasonically cleaned in ethanol. The samples were immersed for 72 h in SBF at a surface area to solution volume ratio (SA/V) of 0.1  $\text{cm}^{-1}$ . After testing, the samples were rinsed with demineralized water and ethanol. The formation of calcium phosphate at the surface of the samples was studied by SEM/EDXA.

Spectrophotometry was used to detect possible release of chromate. Rectangular 3 mm  $\times$  2 mm  $\times$  1 mm Co–Cr–Mo alloy plates were partially coated with glasses G1 and G2. Plates of each type were then immersed in SBF at a SA/V of 0.1  $\text{cm}^{-1}$  for 1 h. The absorbance was measured from 500 to 200 nm and compared with the absorbance of SBF containing 10 ppm  $\text{K}_2\text{CrO}_4$ . Pure SBF was used as reference.

### 3. Results

#### 3.1. Development of firing scheme

##### 3.1.1. Ground coat G1–cover coat C1

Pulverized G1 and C1 glass was fired on platinum foil at 580–700 °C for 20–60 min. Phase separation was observed as a change in colour towards pink. This was more pronounced the higher the firing temperature and the longer the time. The phase separation did not in any case significantly retard sintering. A good result with respect to sintering was achieved by firing G1 at 680 °C for 20–50 min and C1 at 640 °C for 30 min. Thus, on the Co–Cr–Mo-alloy the ground coat was fired at 680 °C for 20 min and the cover coat at 640 °C for 30 min. No cracks were seen by SEM in the coating or between coating and alloy. EDXA of cross-sections showed that aluminium from the ground coat diffused about 5 µm into the cover coat (Fig. 1).

##### 3.1.2. Ground coat G2–cover coat C2

Pulverized G2 and C2 glass was heat-treated for 10 min at temperatures ranging from 570 to 750 °C. Glass G2 did not show signs of crystallization within this temperature range, and sintered well at 750 °C. Glass C2 sintered poorly at all investigated temperatures, leaving pores 5–10 µm in diameter. Below 700 °C the viscous flow was slow and at 700–750 °C crystallization retarded sintering as confirmed by DTA (Fig. 2). Increasing the firing time at 700 °C to 20 min gave a slightly denser coat. A further increase in time did not improve the result. Thus, Co–Cr–Mo specimens were coated by firing G2 at 750 °C for 10 min and C2 at 700 °C for 20 min. No cracks were seen by SEM in the coating or between coating and alloy. EDXA of cross-sections showed that aluminium from the ground coat diffused about 10 µm into the cover coat.

#### 3.2. *In vitro* testing of bioactivity

Bulk specimens and coated alloy specimens (Table II) were studied by SEM/EDXA after immersion for 72 h in SBF. A covering calcium phosphate surface layer characteristic of bioactive glasses, developed on the bulk specimens. When coating the alloy with only a 5 µm thick bioactive cover coat C1 or C2, no calcium phosphate formed upon immersion in SBF. The double coatings G1 + C1 (Fig. 3) and G2 + C2 (Fig. 4) both developed a Si-rich surface layer partly covered by calcium phosphate. EDX analysis of the Ca,P-rich layer gave for G1 + C1 a Ca/P molar ratio of about 1.5 and for G2 + C2 a ratio of 1.2.

#### 3.3. Spectrophotometric analysis

Immediately after immersion of coated samples in SBF, a yellow discoloration of the solution was observed. The coloration was strong at the margin between non-coated and coated metal. When the solution was replenished the colour reaction did not occur again. Spectrophotometric analysis gave a good match to SBF containing K<sub>2</sub>CrO<sub>4</sub> (Fig. 5).

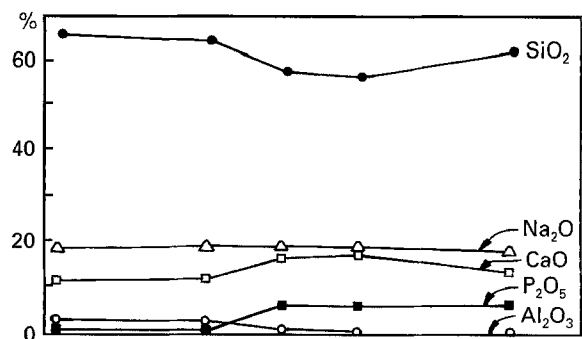


Figure 1 Composition profiles (by EDXA) at the interface between G1 (left) and C1 (right). A slight mixing of the glasses has occurred as seen especially in the Al<sub>2</sub>O<sub>3</sub> and P<sub>2</sub>O<sub>5</sub> profiles.

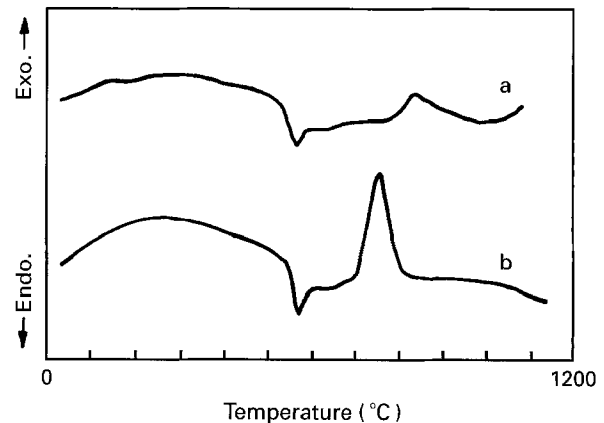


Figure 2 DTA curves for (a) glass G2 and (b) glass C2. For G2, the exothermic crystallization peak starts at a temperature higher than the firing temperature of 750 °C. For C2, crystallization is detected at about 680 °C, i.e. below the firing temperature.

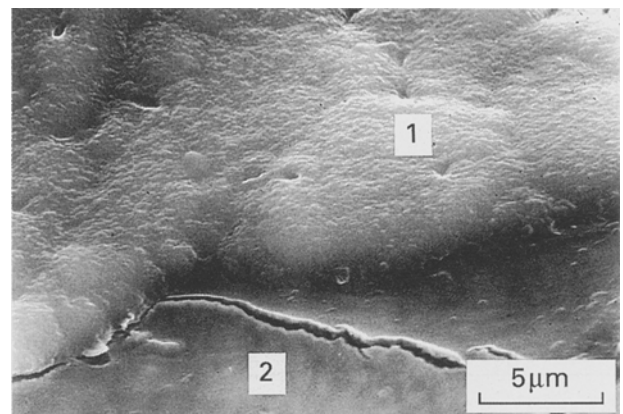


Figure 3 SEM image of G1 + C1-coated Co–Cr–Mo alloy after 72 h in SBF. Compositions by EDXA in indicated spots: (1) SiO<sub>2</sub>, 9.3; Na<sub>2</sub>O, 3.6; CaO, 46.5; P<sub>2</sub>O<sub>5</sub>, 39.8; Al<sub>2</sub>O<sub>3</sub>, 0.8; (2) SiO<sub>2</sub>, 96.5; Na<sub>2</sub>O, 2.2; CaO, 0.0; P<sub>2</sub>O<sub>5</sub>, 0.2; Al<sub>2</sub>O<sub>3</sub>, 1.1. Calcium phosphate (1) has formed on top of the Si-rich layer (2).

### 4. Discussion

No cracks were seen in the double coatings or between coatings and alloy. Thus, the coefficients of thermal expansion of the glasses seem to be sufficiently close to that of the alloy. It has previously been shown that the mineralization of osteoid may be disturbed when the Al<sub>2</sub>O<sub>3</sub> content of the glass exceeds 1.5 wt% [15]. EDXA of cross-sections showed that aluminium from

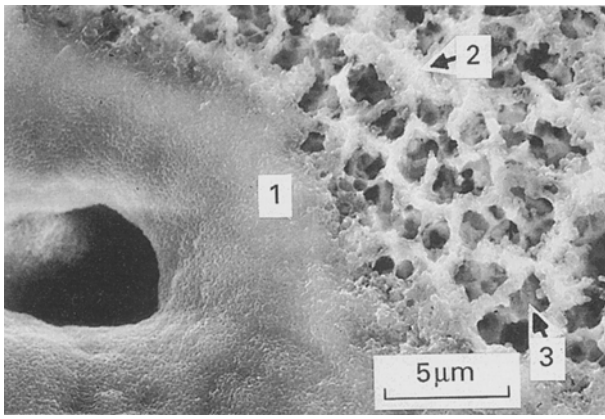


Figure 4 SEM image of G2 + C2-coated Co-Cr-Mo alloy after 72 h in SBF. Compositions by EDXA in indicated spots: (1) SiO<sub>2</sub>, 29.2; Na<sub>2</sub>O, 2.9; CaO, 33.4; P<sub>2</sub>O<sub>5</sub>, 34.1; Al<sub>2</sub>O<sub>3</sub>, 0.4; (2) SiO<sub>2</sub>, 86.9; Na<sub>2</sub>O, 3.8; CaO, 5.7; P<sub>2</sub>O<sub>5</sub>, 2.4; Al<sub>2</sub>O<sub>3</sub>, 1.2. (3) SiO<sub>2</sub>, 90.5; Na<sub>2</sub>O, 2.9; CaO, 3.9; P<sub>2</sub>O<sub>5</sub>, 1.1; Al<sub>2</sub>O<sub>3</sub>, 1.6. Calcium phosphate (1, 2) has formed on top of the open Si-rich layer (3).

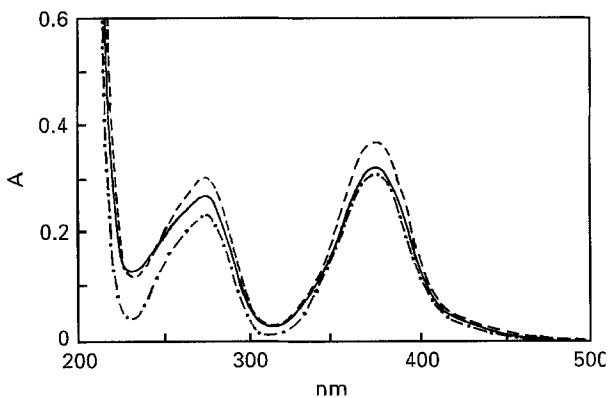


Figure 5 Photometric spectra for (---) SBF after 1 h immersion of G1-coated Co-Cr-Mo alloy; (—) SBF after 1 h immersion of G2-coated Co-Cr-Mo alloy; and (-.-.-) SBF containing 10 ppm K<sub>2</sub>CrO<sub>4</sub>.

the ground coat diffused about 5 μm into the cover coat for G1 + C1 and about 10 μm for G2 + C2. The more extensive mixing in the latter double coating may be due to its higher firing temperatures. The depth of diffusion was taken as the depth at which the Al signal disappeared. Thus, it is possible that aluminium below the detection limit has diffused further into the cover coats. However, the drop in Al<sub>2</sub>O<sub>3</sub> content from the original 3 wt% down to the detection limit occurred over a short distance. This suggests that a zero level is approached rapidly.

Due to crystallization at the firing temperature the cover coat C2 could not be sintered to a dense layer. Pores 5–10 μm in diameter remained. Glass sinters through viscous flow. This process starts when the glass transition temperature is exceeded. The rate of densification increases exponentially with increasing temperature. When the crystallization temperature is reached, the effective viscosity, and thus the densification rate, is determined by the proportions of glass and crystals at the surface. Since the crystals increase the effective viscosity, sintering is retarded. Thus, it is important to develop compositions which do not

crystallize at low temperatures. The present optimization method cannot account for this and further development of the system is desirable.

Immersion of the double coated specimens in SBF resulted in formation of a leached Si-rich layer and on top of this a Ca,P-rich surface layer. This is a characteristic behaviour of bioactive glasses. When optimizing cover coat C2 the phosphate content was fixed at zero and thus, the results agree with previous reports also showing bioactivity for phosphate-free glasses [21, 22]. EDX analysis of the Ca,P-rich layer gave ratios lower than for hydroxylapatite (1.67). This suggests, as does the presence of silica, that the calcium phosphate formation is in its initial stage. Andersson and Kangasniemi reported a Ca/P-ratio of about unity for initially forming calcium phosphate at the surface of a bioactive glass [25]. When coating the alloy with only a 5 μm thick bioactive cover coat C1 or C2, no calcium phosphate formed upon immersion in SBF. As discussed by Hench [13], this can be explained by the dissolution of chromium and/or other metal ions from the alloy into the glass during firing.

Immediately after immersion of the coated samples in SBF, a yellow discoloration of the solution was observed. Yellow colour is characteristic for hexavalent chromium. By comparing the photometric absorbance spectra of the test solutions with that of SBF to which K<sub>2</sub>CrO<sub>4</sub> had been added, the presence of hexavalent chromium was verified. The chromium in the Cr<sub>2</sub>O<sub>3</sub> of the alloy surface is trivalent. For both double coatings calcium phosphate formed, despite the discoloration. Thus, hexavalent chromium in the solution did not inhibit calcium phosphate formation. However, hexavalent chromium is toxic. In its hexavalent state chromium is taken up by red blood cells, whereas trivalent chromium binds to serum proteins [26]. Merritt *et al.* reported that chromium (VI) is released during corrosion of implants [27]. However, in the present study no discoloration was seen in uncoated areas of the alloy. Thus, the presence of glass strongly increased the release of chromium (VI). This is explained by oxidation of chromium (III) to chromium (VI) in the presence of glass. This matter requires further attention since it raises concerns regarding the concept of coating Cr-containing alloys. However, since the discoloration does not re-occur if the SBF is replenished, it seems possible to wash out the chromate prior to implantation. Naturally one must then consider possible effects that the wash might have on the coating.

## 5. Conclusions

When choosing compositions for coating metal implants  $\alpha$ ,  $T_g$ , solubility, and bioactivity can be controlled by the described optimization routine. However, the method does not yet account for crystallization, which may disturb densification of the glass.

Both ground coats were easily densified. Aluminium from the ground coats diffused 5–10 μm into the cover coats. The glasses for cover coats induced formation of calcium phosphate at their surfaces in SBF both as

bulk specimens and as double coatings (G1 + C1, G2 + C2), and are therefore assumed to be bioactive.

When coating a Co–Cr–Mo alloy with only a 5 μm thick bioactive cover coat the bioactivity, as determined by testing in SBF, was lost. This is explained by dissolution of chromium and/or other metal ions into the glass during firing.

Coated Co–Cr–Mo alloy specimens gave a yellow discoloration of SBF. The coloration was strong at the margin between coated and non-coated metal and is due to release of hexavalent chromium. The hexavalent chromium forms due to oxidation of trivalent chromium of the alloy, during firing of the coating. Released hexavalent chromium did not have any notable effect on the calcium phosphate formation at the glass surface.

### Appendix 1. Compositional optimization

Several relations between compositions and properties, such as bioactive response, viscosity, glass transition temperature, solubility, etc. are of the type

$$y = a_0 + \sum a_i x_i^m$$

where  $y$  is the property of interest,  $a_0$  is a constant,  $a_i$  an oxide specific constant,  $x_i$  the fraction of the  $i$ th oxide and  $m$  the power, which mostly is unity. Thus, if  $N_y$  properties are specified, the equation system to be solved contains  $(N_y + 1)$  equations;

$$y_j = a_{0j} + \sum a_{i,j} x_i^m$$

$$\sum x_i = 1$$

where  $y_j$  is the  $j$ th property. The extra equation only specifies that the sum of all oxide fractions is unity.

TABLE III Alternative solutions to the equation system when  $N_y$  is the number of specified properties and  $N_{ox}$  is the number of oxides. The number of solutions indicated is the number of mathematically correct solutions to the equation system

Assumption	Number of solutions	Task
$N_y < N_{ox} - 1$	$\infty$	Find the compositions and choose one
$N_y = N_{ox} - 1$	1	Find the unique composition
$N_y > N_{ox} - 1$	0	Find the composition with the closest fit

Depending on the number of properties specified ( $N_y$ ) and the number of oxides available ( $N_{ox}$ ), the equation system may have one unique solution, it may be underdetermined or it may be overspecified, as summarized in Table III. If the number of specified properties is less than the number of oxides minus one ( $N_y < N_{ox} - 1$ ) the number of solutions is infinite and there is a problem to decide which one to choose. As long as the mathematical answer is inside the compositional validity range of the equations, any of these solutions may be chosen. Further screening may be done by introducing a termination criterion, such as choose the cheapest! The second alternative in Table III gives one unique solution, while no glass composition can be found that meets the specifications when the number of specified properties exceeds the number of oxides minus one (Table III, alternative 3). The best answer is then found by minimizing the sum of square errors. Sometimes this optimization problem is made more relevant by specifying the importance of each property by giving each one a different weight.

TABLE IV Summary of compositional optimization of coatings for a Co–Cr–Mo alloy. The minimum and maximum limits for the compositions are set by the ranges used in developing the models. These limits are Na<sub>2</sub>O, 15.0–30.0; CaO, 10.0–25.0; B<sub>2</sub>O<sub>3</sub>, 0.0–3.0; Al<sub>2</sub>O<sub>3</sub>, 0.0–3.0; SiO<sub>2</sub>, 38.0–65.5 and P<sub>2</sub>O<sub>5</sub>, 0.0–8.0. The limits for the properties are set by the requirements on the compositions. The compositions, given in Table I, were developed to be used in the combinations G1 + C1 and G2 + C2

Properties	Weight factor	Minimum value	Predicted actual value	Maximum value
G1 (ground coat)				
Thermal expansion (10 <sup>-5</sup> K <sup>-1</sup> )	100	1.39	1.39	1.41
Transition temperature (°C)	100	515	517	518
Solubility (0.01 M ml HCl/200 mg glass)	10	0.00	0.00	0.01
Reaction number	10	1.00	2.40	2.40
C1 (cover coat)				
Thermal expansion (10 <sup>-5</sup> K <sup>-1</sup> )	100	1.30	1.39	1.39
Transition temperature (°C)	100	500	520	520
Solubility (0.01 M ml HCl/200 mg glass)	10	0.00	2.14	3.00
Reaction number	100	5.80	5.80	8.00
G2 (ground coat)				
Thermal expansion (10 <sup>-5</sup> K <sup>-1</sup> )	100	1.25	1.27	1.35
Transition temperature (°C)	100	540	535	590
Solubility (0.01 M ml HCl/200 mg glass)	10	0.00	0.61	1.00
Reaction number	100	0.00	0.72	1.00
C2 (cover coat)				
Thermal expansion (10 <sup>-5</sup> K <sup>-1</sup> )	100	1.25	1.29	1.35
Transition temperature (°C)	100	470	542	550
Solubility (0.01 M ml HCl/200 mg glass)	10	0.00	6.251	4.00
Reaction number	100	6.00	5.63	8.00

All mathematically correct solutions (Table III, alternatives 1 and 2) may sometimes be outside the validity ranges of the equations. However, often there is no need to specify a property value exactly. Thus, each property may be given limits within which any value is acceptable. Usually this means that the number of solutions to the problem becomes infinite and the choice of recipe may be done by using a termination criterion, as discussed above. If still no solution is found within the validity ranges of the equations, the situation resembles alternative 3 and the optimization may be done by weighting the properties and minimizing their square errors.

Thus, usually the problem can be treated as one to which several solutions exist. These are all equal as far as the properties are concerned. However, if other criteria are also considered, one of the solutions is usually to be preferred.

The optimization data and the predicted properties for the developed compositions (Table I) are given in Table IV. For glasses G1 and C1 the number of specified properties is less than the number of oxides minus one,  $N_y < N_{ox} - 1$ . For glasses G2 and C2 the  $P_2O_5$  content is fixed at zero and  $N_y = N_{ox} - 1$ . The properties were specified within certain limits and in order to account for the possibility of no solution within the compositional validity ranges of the equations, the properties were given different weights. Thus, there may be other compositions which equally well as the chosen ones, give the required properties.

## References

1. D. C. GREENSPAN and L. L. HENCH, *J. Biomed. Mater. Res. Symp.* **7** (1976) 503.
2. J. E. RITTER Jr, D. C. GREENSPAN, R. A. PALMER and L. L. HENCH, *J. Biomed. Mater. Res.* **13** (1979) 251.
3. P. GRISS, D. C. GREENSPAN, G. HEIMKE, B. KREMPIEN, R. BUCHINGER, L. L. HENCH and G. JENTSCHURA, *J. Biomed. Mater. Res. Symp.* **7** (1976) 511.
4. L. L. HENCH, C. G. PANTANO, P. J. BUSCEMI and D. C. GREENSPAN, *J. Biomed. Mater. Res.* **11** (1977) 267.
5. G. PIOTROWSKI, L. L. HENCH, W. C. ALLEN and G. J. MILLER, *J. Biomed. Mater. Res. Symp.* **6** (1975) 47.
6. P. DUCHEYNE, L. L. HENCH, A. KAGAN, M. MARTENS and J. C. MULIER, *Arch. Orthop. Traumat. Surg.* **94** (1979) 155.
7. E. SCHEPERS, P. DUCHEYNE and M. DE CLERCQ, *J. Biomed. Mater. Res.* **23** (1989) 735.
8. A. KRAJEWSKI, A. RAVAGLIOLI, R. VALMORI, S. STURLESE and S. M. INGO, *J. Mater. Sci.* **21** (1986) 1625.
9. W. R. LACEFIELD and L. L. HENCH, *Biomaterials* **7** (1986) 104.
10. G. A. FUCHS and K. DEUTSCHER, *Arch. Orthop. Traumat. Surg.* **98** (1981) 121.
11. P. DUCHEYNE, A. BURSSSENS and M. MARTENS, *J. Biomed. Mater. Res.* **18** (1984) 1017.
12. J. K. WEST, A. E. CLARK, M. B. HALL and G. E. TURNER, in: "CRC handbook of bioactive ceramics", Vol. 1, edited by T. Yamamuro, L. L. Hench and J. Wilson (CRC Press, Boca Raton, 1990) p. 161.
13. L. L. HENCH, in: "CRC handbook of bioactive ceramics", Vol. 1, edited by T. Yamamuro, L. L. Hench and J. Wilson (CRC Press, Boca Raton, 1990) p. 7.
14. U. M. GROSS and V. STRUNZ, *J. Biomed. Mater. Res.* **19** (1985) 251.
15. Ö. H. ANDERSSON, K. H. KARLSSON, K. KANGASNIEMI and A. YLI-URPO, *Glastech. Ber.* **61** (1988) 300.
16. Ö. H. ANDERSSON, G. LIU, K. H. KARLSSON, L. NIEMI, J. MIETTINEN and J. JUHANOJA, *J. Mater. Sci. Mater. Med.* **1** (1990) 219.
17. T. WESTERLUND, L. HATAKKA and K. H. KARLSSON, *J. Amer. Ceram. Soc.* **66** (1983) 574.
18. L. HATAKKA and K. H. KARLSSON, *Glass Technol.* **27** (1986) 17.
19. H. KALSING, *Sprechsaal* **88** (1955) 193, 540.
20. Ö. H. ANDERSSON, *J. Mater. Sci. Mater. Med.* **3** (1992) 326.
21. Ö. H. ANDERSSON, G. LIU, K. KANGASNIEMI and J. JUHANOJA, *ibid.* **3** (1992) 145.
22. Ö. H. ANDERSSON, K. H. KARLSSON and K. KANGASNIEMI, *J. Non-Cryst. Solids* **119** (1990) 290.
23. T. KOKUBO, H. KUSHITANI, S. SAKKA, T. KITSUGI and T. YAMAMURO, *J. Biomed. Mater. Res.* **24** (1990) 721.
24. J. GAMBLE, "Chemical anatomy, physiology and pathology of extracellular fluid", 6th edn (Harvard University Press, Cambridge, MA, 1967) p. 1.
25. Ö. H. ANDERSSON and I. KANGASNIEMI, *J. Biomed. Mater. Res.* **25** (1991) 1019.
26. S. J. GRAY and K. STERLING, *J. Clin. Invest.* **29** (1950) 1604.
27. K. MERRIT and S. A. BROWN, in "Biomaterials and biomechanics", edited by P. Ducheyne, G. V. der Perre and A. E. Aubert (Elsevier, Amsterdam, 1983) p. 221.

Received 12 October 1993  
and accepted 10 October 1994